Ab initio calculations and analysis of the torsional spectra of dimethylamine and dimethylphosphine

M. Luisa Senent and Yves G. Smeyers

Citation: J. Chem. Phys. **105**, 2789 (1996); doi: 10.1063/1.472141

View online: http://dx.doi.org/10.1063/1.472141

View Table of Contents: http://jcp.aip.org/resource/1/JCPSA6/v105/i7

Published by the American Institute of Physics.

Ab initio calculations and analysis of the torsional spectra of dimethylamine and dimethylphosphine

M. Luisa Senent and Yves G. Smeyers
Instituto de Estructura de la Materia, CSIC, calle Serrano, No 123, E-28006 Madrid, Spain

(Received 15 April 1996; accepted 10 May 1996)

In the present paper, *ab initio* calculations at MP2/RHF level are performed with different basis sets 6-31G(d,p), 6-311G(d,p), and 6-311(df,p) to determine the potential energy functions, the kinetic parameters, and the dipole moment components as a function of the double methyl rotation in dimethylamine (DMA) and dimethylphosphine (DMP). From the potential energy and kinetic parameters, the torsional energy levels and torsional functions are determined, and from the dipole moment variations, the far infrared spectra are synthesized by calculating both the frequencies and the intensities. The results are in relatively good agreement with experimental spectra. Calculations confirm the assignments performed with the experimental potentials fitted with only five terms. The calculations, however, allow to reassign the observed band at 239.8 cm^{-1} in DMA and at 177.2 cm^{-1} in DMP to the superimposition of two different transitions: the 03→04 third sequence and an 10→11 vibrationally excited fundamental. © *1996 American Institute of Physics.* [S0021-9606(96)03231-X]

I. INTRODUCTION

The analysis of the far infrared patterns of dimethylamine[1] (DMA) and dimethylphosphine[2,3] (DMP) shows an unusual complexity since the two torsional modes a' and a'' are active in infrared. Both sets of transitions lie in the same region of the spectrum giving rise to bc-hybrid and a-type bands. These bands show a prominent Q branch and their assignments require the comparative study of the Raman and FIR spectra. In DMA, furthermore, the bands due to the bending mode appear in the same region as those of two torsional overtones. In exchange, several torsional bands of vibrationally excited states of the CNC bending mode appear also in the same zone.

The torsional frequencies, structures and barriers of DMA[1,4–15] and DMP[2–3,16–21] have been considered in many papers. In 1967, Fateley *et al.*[6] and Möller *et al.*[7] have first observed the torsional spectrum of DMA. They have found barrier heights of 1150 and 1266 cm^{-1}. Later, in 1971, Wollrab *et al.*[9,10] have obtained a barrier of 1126.2 cm^{-1} from microwave data. The most relevant analysis of the IR and Raman structures of DMA is due to Durig, Griffin, and Groner,[1] who have evaluated, in 1977, a torsional barrier of 1053.8 cm^{-1}. As is expected, the barrier height was found to possess approximately an intermediate value between those of methylamine[22] (714.6 cm^{-1}) and trimethylamine[23] (1538.9 cm^{-1}). Finally, Consalvo *et al.*[15] have also considered the Raman spectra of DMA.

The most relevant experiments for DMP are due to Durig, Griffin, and Natter,[2] and Durig, Groner, and Li.[3] Durig *et al.*[2,3] have evaluated a barrier height of 700.8 cm^{-1} from IR and Raman spectroscopies and of 811.0 cm^{-1} from MW data. This barrier shows also an intermediate value between those of methylphosphine[24] and trimethylphosphine.[23]

Fully and partially optimized *ab initio* calculations can be applied to verify the assignment of IR and Raman spectra. This technique was first employed for a set of molecules showing the G_{36} symmetry and two C_{3v} symmetrical rotors such as thioacetone,[25] acetone,[26] biacetyl,[27] dimethyl-ether,[28,29] dimethyl-sulphide,[30] and butenes.[31] For that purpose, two and three dimension models were used. In the present paper, we applied the same technique to study the internal rotation in DMA and DMP, assuming that the torsional coordinates could be separated from those of the others vibration modes. The CNC (or CPC) bending and the hydrogen inversion modes, however, are expected to interact strongly with the two torsional modes in the amine or phosphine groups. The potential energy interactions are partially introduced in the geometry optimization. With this restriction, the two molecules can be classified according to the G_{18} nonrigid group.[32–34]

The minimal analytic expression[32–34] of the restricted torsional potentials of the G_{18} molecules is a ten term symmetry adapted Fourier expansion. Experimental data, however, allows only the fitting of five term functions into the G_{36} symmetry. The incidence of the remaining terms on the frequencies could be evaluated by performing *ab initio* calculations. In order to estimate these effects, the torsional levels were evaluated theoretically by using ten and seven termed expansions. For these purposes, different basis sets and approximations for the electronic correlation were resorted.

II. THEORY

By assuming the separability of large amplitude vibrations, the molecules of DMA and DMP may be described as a rigid C_s frame and two C_{3v} symmetric tops. Thus, the two-dimensional structure may be classified according to the G_{18} r-NRG group. At the lowest energy levels, where the tops undergo torsional oscillations, two vibrational normal modes, in which the torsion occurs in the same or opposite sense, may be defined. They can be classified into the a' and a'' representations of the C_s point group. Both modes are

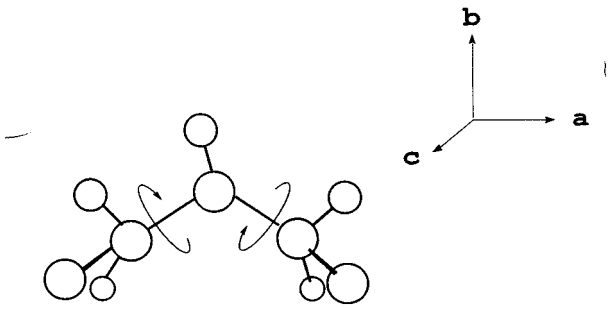

FIG. 1. The molecular structure of dimethylamine, the symmetry axes and the torsional angles θ_1 and θ_2.

active in IR. Figure 1 shows the molecule of DMA, as well as the symmetry axis x, y, and z. The sense of the rotation of both methyl groups is defined clockwise.

The torsional Hamiltonian may be written as[26]

$$\hat{H}(\theta_1,\theta_2) = -\frac{\partial}{\partial\theta_1} B_{11} \frac{\partial}{\partial\theta_1} - \frac{\partial}{\partial\theta_1} B_{12} \frac{\partial}{\partial\theta_2} - \frac{\partial}{\partial\theta_2} B_{12} \frac{\partial}{\partial\theta_1} - \frac{\partial}{\partial\theta_2} B_{22} \frac{\partial}{\partial\theta_2} + V(\theta_1,\theta_2),$$

where $B_1(\theta_1,\theta_2)$, $B_2(\theta_1,\theta_2)$, and $B_{12}(\theta_1,\theta_2)$ are the kinetic parameters and $V(\theta_1,\theta_2)$ is the potential energy function. Both types of parameters depend on the two torsional angles. The analytic expression for them is a ten term double Fourier expansion.[32–34] The first seven terms are totally symmetric with respect to the exchange of the two torsional angles:

$$\begin{aligned} V(\theta_1,\theta_2) &= \sum_{L>K}^{2}\sum_{K=0}^{1} A_{KL}^{cc}[\cos 3K\theta_1 \cos 3L\theta_2 \\ &+ \cos 3L\theta_1 \cos 3K\theta_2] + \sum_{K}^{2} (A_{KK}^{cc} \cos 3K\theta_1 \\ &\times \cos 3K\theta_2) + \sum_{K}^{1} A_{KK}^{ss} (\sin 3K\theta_1 \sin 3K\theta_2) \\ &+ \sum_{K=0}^{2} A_K^{cs}[\cos 3K\theta_1 \sin 3\theta_2 - \sin 3\theta_1 \cos 3K\theta_2]. \end{aligned}$$

The last three are antisymmetric. Both types of terms, however, are invariant with respect to the double-switch-exchange operation, WV.

The r-NRG[34] G_{18} contains all the symmetry operations that commute with the torsional Hamiltonian. This group can be defined by the products

$$G_{18} = [C_3^I \otimes C_{3'}^I] \wedge [WV^I],$$

where the subgroups are defined as

$$C_3^I = [\hat{E} + \hat{C}_3 + \hat{C}_3^2], \quad WV^I = [\hat{E} + \hat{W}\hat{V}]$$

and $\hat{C}_3$ and $\hat{W}\hat{V}$ are the rotation and double-switch-exchange operators, respectively. This last operation is defined by the expression:

$$\hat{W}\hat{V} f(\theta_1,\theta_2) = f(-\theta_2,-\theta_1).$$

Table I shows the character table of the G_{18} group.[33] This group contains six symmetry species. The nondegenerate A_1 and A_2 are symmetric and antisymmetric with respect to the double-switch-exchange operation. The pseudo-degenerate representations E_1 and E_2 include a complex conjugate pair of one-degenerate representations (E_{1a} and E_{1b}, E_{2a} and E_{2b}). E_3 is a two-degenerate representation and G contains a complex conjugate pair of two-degenerate representations (G_{1a}, G_{1b}, G_{2a}, and G_{2b}).

The nuclear Hamiltonian is solved variationally by expanding the solutions onto the basis of the symmetry eigenvectors, which factorize the Hamiltonian matrix in eight boxes. Six correspond to the A_1, A_2, G_1, G_2, E_1, and E_2 representations and two to the E_3 two-degenerate specie. Boxes containing pseudo-degenerate representations cannot be factorized without including the wagging coordinate as a third degree of freedom. The symmetry eigenvectors for the G_{18} group may be determined from those of G_{36} group developed for the analysis of the torsional spectra of acetone.[35] Thus, the set of eigenvectors for the A_1 representations contains the A_1 and A_2 ones of the G_{36} group. In the same way, the G_{18} representations A_2 and E_3 can be related to the A_3 and A_4, and E_{3x} and E_{4y} representations of the G_{36} group. The vectors for the pseudo-degenerate representations G_1, G_2, E_1, and E_2 can be obtained from the G_1 and G_2, G_3 and G_4, E_{1x} and E_{1y}, and E_{2x} and E_{2y} of the G_{36} group.

TABLE I. Character table of the G_{18} r-NRG.[a]

	$\hat{E}$	$\hat{C}_{3'}^2$, C_3	$\hat{C}_3^2$, $\hat{C}_{3'}$	$2\hat{C}_3\hat{C}_{3'}$	$\hat{C}_3\hat{C}_{3'}^2$,	$\hat{C}_3^2\hat{C}_{3'}$	$\hat{W}\hat{V}$, $\hat{W}\hat{V}\hat{C}_3^2\hat{C}_{3'}^2$, $\hat{W}\hat{V}\hat{C}_3\hat{C}_{3'}$,	$\hat{W}\hat{V}C_3C_{3'}^2$, $\hat{W}\hat{V}\hat{C}_{3'}^2$, $\hat{W}\hat{V}C_3$	$\hat{W}\hat{V}\hat{C}_3^2\hat{C}_{3'}$, $\hat{W}\hat{V}\hat{C}_3^2$ $\hat{W}\hat{V}\hat{C}_{3'}$,
A_1	1	1	1	1	1	1	1	1	1
A_2	1	1	1	1	1	1	−1	−1	−1
E_{1a}	1	ω^2	ω	1	ω^2	ω	1	ω^2	ω
E_{1b}	1	ω	ω^2	1	ω	ω^2	1	ω	ω^2
E_{2a}	1	ω^2	ω	1	ω^2	ω	−1	$-\omega^2$	$-\omega$
E_{2b}	1	ω	ω^2	1	ω	ω^2	−1	$-\omega$	$-\omega^2$
E_3	2	−1	−1	−1	2	2	0	0	0
G_{1a}	2	$-\omega^2$	$-\omega$	−1	$2\omega^2$	2ω	0	0	0
G_{1b}	2	$-\omega$	$-\omega^2$	−1	2ω	$2\omega^2$	0	0	0

[a] $\overline{\omega} = \exp(2\pi i/3)$.

TABLE II. Selection rules for DMA and DMP.

FIR Raman	$\mu_x\ \mu_y$ $\alpha_{xx},\alpha_{yy},\alpha_{zz}$	μ_z
	$A_1 \rightleftarrows A_1$	$A_1 \rightleftarrows A_2$
	$A_2 \rightleftarrows A_2$	
	$G \rightleftarrows G$	$G \rightleftarrows G$
	$E_1 \rightleftarrows E_1$	$E_1 \rightleftarrows E_2$
	$E_2 \rightleftarrows E_2$	
	$E_3 \rightleftarrows E_3$	$E_3 \rightleftarrows E_3$

The intensities of each type of bands are determined into the electric dipole moment variation approximation. In this aim, the intensity equation adapted for a two symmetric top problem[36] is used:

$$f_{fi}=\frac{g}{3B}\,(E_f-E_i)(C_f-C_i)\langle\psi_i|\,\frac{\mu(\theta_1,\theta_2)}{\mathrm{Re}}\,|\psi_j\rangle^2.$$

In this expression, E_f, E_i, C_f, C_i, ψ_f, and ψ_i are the energies, populations, and torsional wave functions of the final and initial states, respectively. $\mu(\theta_1,\theta_2)$ is the dipole moment vector expressed as a function of the rotation angles. g is the nuclear statistical weight, R and B are the average rotation radius and kinetic parameter of a methyl group, and e the elemental electric charge.

The electric dipole moment components μ_z, μ_y, and μ_x with respect to the principle axis a, b, and c, have to be deduced from the *ab initio* calculations. It is easy to verify that these components transform according to the A_2, A_1, and A_1 representations of the G_{18} group. In Table II, the selection rules obtained from the nonzero conditions of the transitions moments, are given. Because of the vectorial nature of the spin functions, the nuclear statistical weights for each symmetry coincide with those determined for the G_{36} molecules.[26] Finally, the populations are given by a Boltzmann statistics.

III. CALCULATIONS

Fully optimized *ab initio* calculations were performed at the MP2/RHF level with the program GAUSSIAN 92.[37] Torsional energies, frequencies and intensities were determined with the program ROCA25 especially written for this paper. The potential energy functions were calculated by fitting the relative electronic energy values (with respect to the minima) of ten selected conformations to Eq. (2). In Table III, these relative electronic energies calculated with 6-31G(d,p), 6-311G(d,p), and 6-311G(df,p) are given. The angles $\theta_1=0.0$ *y* $\theta_2=0.0$ correspond to the planar conformation in which two of the hydrogens are lying on the CNC (CPC) plane and pointing outward. The relative energies for these conformations were determined to be 33.588 cm^{-1} in DMA and 149.776 cm^{-1} in DMP [MP2/6-31G(df,p)]. Table III shows also the effective barrier height (saddle-point) and the maxima of the surface, as well as the conformational angles of the minima. In Table IV, the expansion coefficients of the potential energy functions are given.

The minimum energy conformation of DMA shows torsion angles of $\theta_1=3.3°$ and $\theta_2=-3.3°$ [MP2/6-311G(df,p)]. The wagging and bending coordinates at this equilibrium geometry were found to be equal to 55° and 111.6°, respectively. The C–H and N–H bond distances were found to be 1.449 and 1.012 Å. The minimum energy conformation of DMP possesses torsion angles of $\theta_1=10.8°$ and $\theta_2=-10.8°$. The bending and wagging angles of this structure were found to be 99.9° and 67°. The values for the C–P and P–H bond distances are equal to 1.84 and 1.41 Å. The separation be-

TABLE III. Relative energies (in cm^{-1}) with respect to the equilibrium geometry at the MP2/RHF approximation.

		DMA[a]			DMP[a]		
θ_1^b	θ_2^v	I	II	III	I	II	III
0.0	0.0	39.967	40.320	33.588	150.362	151.356	149.776
60.0	0.0	1259.180	1222.850	1197.378	770.059	731.396	747.963
60.0	60.0	2385.832	2372.815	2334.771	1506.754	1480.753	1536.449
30.0	0.0	766.030	743.204	710.012	704.215	677.945	684.424
60.0	30.0	1661.300	1626.821	1614.142	865.429	829.613	860.862
30.0	30.0	1213.572	1174.133	1148.663	760.542	717.255	731.962
30.0	−30.0	1418.349	1414.472	1356.711	1349.330	1331.405	1356.750
0.0	30.0	454.536	425.325	423.462	203.830	180.321	183.978
30.0	60.0	1951.405	1936.607	1884.283	1413.513	1381.757	1417.870
−30.0	30.0	861.653	836.060	848.160	297.289	277.826	293.521
V_{eff}		1263.578	1228.356	1201.238	762.117	726.434	744.954
Maximum		2420.453	2412.709	2364.790	1690.390	1672.736	1727.413
Equilibrium structure							
$\theta_1=-\theta_2$		3.6	4.0	3.3	10.9	11.1	10.8
Total energy[c]		−134.737 67	−134.829 33	−134.875 40	−420.974 01	−420.172 56	−420.220 11

[a]Basis set I(6-31G(d,p); basis set II=6-311G(d,p); basis set III=6-311G(df,p).
[b]In degrees.
[c]In a.u.

TABLE IV. Calculated expansion coefficients for the potential energy in dimetylamine and dimethylphosphine[a].

	DMA[b]			DMP[b]		
	V_1	V_2	V_3	V_1	V_2	V_3
A_{00}^{cc}	1207.112	1181.297	1157.792	796.492	767.277	786.656
A_{10}^{cc}	−609.461	−609.682	−597.945	−427.789	−424.612	−437.577
A_{11}^{cc}	−26.676	−11.001	−9.422	41.539	54.967	59.376
A_{20}^{cc}	15.612	18.061	17.091	4.298	7.436	9.124
A_{21}^{cc}	4.347	6.505	6.747	5.192	6.428	5.723
A_{22}^{cc}	−1.434	−0.064	−0.157	−1.432	−0.748	−0.573
A_{11}^{ss}	34.433	21.328	21.202	−20.057	−30.558	−33.680
A_{01}^{cs}	−30.237	−25.673	−30.894	−37.482	−35.024	−35.068
A_{11}^{cs}	−7.334	−5.032	−6.496	4.806	5.872	5.686
A_{21}^{cs}	−6.960	−8.127	−7.676	−1.113	−2.267	−1.196

[a]In cm^{-1}.
[b]V_1 from MP2/6-31G(d,p) energies; v_2 from MP2/6-311G(d,p); v_3 from MP2/6-311G(df,p) energies.

tween the methyl hydrogen atoms appears to be larger in DMP than in DMA. The variations of the coordinates with the torsion are weaker in DMP than in DMA, since the steric interactions are smaller.

The kinetic parameters were determined for each conformation from the optimized geometries. For this purpose, the derivatives of the Cartesian coordinates with respect to the torsional coordinates were calculated numerically. In Table V, the expansion coefficients of the kinetic functions, obtained by fitting the parameters for each structure to a symmetry adapted Fourier expansion, are given.

The torsional energy levels were determined by using six different potentials of G_{36} and G_{18} symmetries obtained by using three different basis set in the electronic calculations. The G_{36} potential and the G_{36} kinetic parameters were determined from the G_{18} functions of Tables IV and V by dropping the nonsymmetric terms with respect to the exchange operator. An accurate variational calculation of the levels requires 37×37 torsional basis functions. Thus, the Hamiltonian matrix factorizes in eight boxes of dimensions: $A_1(91)$, $A_2(78)$, $G(2\times312)$, $E_1(156)$, $E_2(132)$, and $E_3(2\times144)$. Boxes G, E_1, and E_2 contain two pseudodegenerate and inseparable representations. Table VI shows the levels for both molecules obtained with four of these potentials and classified according to the vibrational quanta and the symmetry species of the G_{36} and G_{18} groups. In Tables VII, the calculated and observed band positions are given.

For the intensities,[36] the values of the dipole moment components, obtained for each conformation at the RHF/6-311(df,p) level, were retained and fitted to A_2, A_1, and A_1 symmetry adapted Fourier expansions. Intensities for the inseparable degenerate species were the sums of those of the separate allowed transitions. The $G-G$ transitions were found to be the most intense because of the effect of the nuclear statistical weights. These intensities are given in Table VIII.

The rotational contours[38] of the bands were simulated from the expectation values of the A, B, and C rotational constants at the two first A_1 levels as well as at the first A_2. Figures 2 and 3 show a plot of the calculated rotational structures corresponding to bc-hybrid and a-type bands. Both

TABLE V. Expansion coefficients for the kinetic energy.[a]

	MP2/6-31G(d,p)		MP2/6-311G(d,p)		MP2/6-311G(df,p)	
	B_1	B_{12}	B_1	B_{12}	B_1	B_{12}
DMA[b]						
A_{00}^{cc}	6.696	−1.111	6.626	−1.090	6.651	−1.110
A_{10}^{cc}	−0.054	0.051	−0.051	0.048	−0.053	0.050
A_{11}^{cc}	0.020	−0.024	0.016	−0.021	0.019	−0.023
A_{11}^{ss}	−0.027	0.032	−0.025	0.030	−0.027	0.032
A_{01}^{cs}	−0.020	0.021	−0.016	0.016	−0.019	0.019
DMP[c]						
A_{00}^{cc}	5.856	−0.259	5.805	−0.255	5.812	−0.262
A_{10}^{cc}	−0.011	0.009	−0.012	0.010	−0.013	0.010
A_{11}^{cc}	0.006	−0.006	0.006	−0.006	0.006	−0.007
A_{11}^{ss}	−0.007	0.008	−0.007	0.009	−0.083	0.008
A_{01}^{cs}	0.003	−0.006	0.003	−0.005	0.031	−0.005

[a]In cm^{-1}.
[b]Experimental values are $B_1=B_2=6.622$ cm^{-1} and $B_{12}=-1.115$ cm^{-1}.
[c]Experimental values are $B1=B2=5.728$ cm^{-1} and $B_{12}=-0.255$ cm^{-1}.

TABLE VI. (a) Dimethylamine and (b) dimethylphosphine energy levels.[a]

		$V_3(G_{36})$		$V_1(G_{18})$	$V_2(G_{18})$	$V_3(G_{18})$
(a)						
0 0	A_1	240.392	A_1	248.791	240.454	237.541
	G	240.392	G	248.791	240.454	237.541
	E_1	240.392	E_1	248.791	240.454	237.541
	E_3	240.392	E_3	248.791	240.454	237.541
1 0	A_3	461.562	A_2	481.603	463.867	458.767
	G	461.561	G	481.602	463.867	458.766
	E_2	461.560	E_2	481.602	463.866	458.765
	E_3	461.560	E_3	481.602	463.866	458.765
0 1	A_2	491.478	A_1	509.064	494.859	490.330
	G	491.477	G	509.064	494.859	490.329
	E_1	491.476	E_1	509.064	494.858	490.328
	E_4	491.476	E_3	509.064	494.858	490.328
2 0	A_1	677.741	A_1	707.107	682.433	675.153
	G	677.759	G	707.123	682.448	675.170
	E_1	677.778	E_1	707.138	682.464	675.188
	E_3	677.778	E_3	707.138	682.464	675.188
1 1	A_4	701.276	A_2	729.945	707.152	700.143
	G	701.304	G	729.968	707.176	700.171
	E_2	701.332	E_2	729.991	707.200	700.198
	E_4	701.332	E_3	729.991	707.200	700.198
0 2	A_1	739.400	A_1	763.525	745.222	738.909
	G	739.409	G	763.532	745.230	738.918
	E_1	739.418	E_1	763.539	745.238	738.927
	E_3	739.418	E_3	763.539	745.238	738.927
3 0	A_3	887.090	A_2	923.897	894.329	884.838
	G	886.907	G	923.753	894.182	884.663
	E_2	886.729	E_2	923.613	894.040	884.493
	E_3	886.729	E_3	923.613	894.040	884.493
2 1	A_2	903.181	A_1	940.348	911.629	902.170
	G	902.854	G	940.092	911.357	901.849
	E_1	902.523	E_1	939.834	911.082	901.525
	E_4	902.523	E_3	939.834	911.082	901.525
1 2	A_3	937.734	A_2	972.710	946.199	937.202
	G	937.571	G	972.595	946.060	937.038
	E_2	937.407	E_2	972.479	945.918	936.872
	E_3	937.406	E_3	972.479	945.918	936.872
0 3	A_2	982.308	A_1	1011.478	990.273	982.045
	G	982.287	G	1011.470	990.256	982.024
	E_1	982.266	E_1	1011.463	990.239	982.003
	E_4	982.266	E_3	1011.463	990.239	982.003
(b)						
0 0	A_1	179.505	A_1	184.902	175.592	177.339
	G	179.505	G	184.902	175.592	177.340
	E_1	179.506	E_1	184.903	175.593	177.340
	E_3	179.506	E_3	184.903	175.593	177.340
1 0	A_3	345.013	A_2	359.855	340.440	343.268
	G	345.003	G	359.846	340.429	343.258
	E_2	344.993	E_2	359.837	340.418	343.249
	E_3	344.993	E_3	359.837	340.418	343.249
0 1	A_2	367.201	A_1	376.200	361.209	365.437
	G	367.190	G	376.191	361.196	365.427
	E_1	367.179	E_1	376.181	361.184	365.415
	E_4	367.179	E_3	376.181	361.184	365.415
2 0	A_1	510.287	A_1	530.442	504.459	508.916
	G	510.406	G	530.572	504.597	509.034
	E_1	510.530	E_1	530.712	504.743	509.157
	E_3	510.530	E_3	530.712	504.743	509.157
1 1	A_4	518.943	A_2	535.907	511.788	517.494
	G	519.146	G	536.107	512.018	517.695
	E_2	519.345	E_2	536.299	512.240	517.891
	E_4	519.345	E_3	536.299	512.240	517.891
0 2	A_1	552.637	A_1	564.212	544.443	551.170
	G	552.711	G	564.262	544.521	551.243
	E_1	552.785	E_1	564.313	544.599	551.316
	E_3	552.785	E_3	564.313	544.599	551.316
2 1	A_2	669.439	A_1	689.951	660.753	668.235
	G	665.800	G	686.144	656.806	664.635
	E_1	665.576	E_1	685.854	656.402	664.396
	E_4	665.576	E_3	685.853	656.401	664.395
3 0	A_3	669.496	A_2	690.430	661.351	668.344
	G	669.470	G	690.210	661.086	668.295
	E_2	666.033	E_2	686.475	657.279	664.887
	E_3	666.034	E_3	686.475	657.280	664.888
1 2	A_3	697.148	A_2	718.157	688.600	696.055
	G	696.767	G	718.029	688.294	695.686
	E_2	696.385	E_2	717.901	687.989	695.318
	E_3	696.385	E_3	717.901	687.989	695.318
0 3	A_2	733.976	A_1	746.434	723.291	732.735
	G	733.784	G	746.378	723.114	732.547
	E_1	733.588	E_1	746.321	722.933	732.355
	E_4	733.588	E_3	746.321	722.933	732.355

[a]In cm^{-1}.

contours show a prominent Q branch. The Q branch of the hybrid structure is due from the c-type component.

IV. ASSIGNMENT AND DISCUSSION

Assignments of the Q branches have to be accomplished from the calculations and from the comparative analysis of the Raman and FIR spectra.[1–3] From the rotational band profiles in Figs. 2 and 3, it is clear that the bc-hybrid and a-type bands have sharp Q branches. Transitions attached to the a' mode are active in Raman, whereas the a'' transitions are nonactive. The pattern observed in the FIR spectrum of DMA between 235.0 and 256.3 cm^{-1} (see Fig. 4) is also visible in the Raman spectrum. Thus, it has to be assigned to the a' mode. Furthermore, bands observed between 202 and 220 cm^{-1} should be assigned to a'' mode. In DMP spectrum (see Fig. 5), four of the six recorded bands can be assigned to the a' mode. Calculations support this assignment.

The fundamental transitions present the strongest intensities (see Table VIII). They correspond to the sharpest bands of each symmetry. In DMA, the most prominent bands of each pattern were observed at 256.3 and 219.4 cm^{-1}. They were predicted theoretically at 252.788 and 221.225 cm^{-1} into the MP2/6-311G(df,p) approximation. In DMP, the two bands were observed at 190.4 and 169.9 cm^{-1} and they were predicted at 188.087 and 165.918 cm^{-1} at the same level of approximation. The separation between the two fundamentals of DMA was observed and calculated to be 36.9 and 31.563 cm^{-1}, respectively. In DMP, 20.5 and 22.169 cm^{-1}.

Divergences between the experimental and calculated values for the fundamental frequencies arise from the potential energy parameters rather than the kinetic parameters, since they were calculated accurately and are in agreement with the experimental data.[1–3] In DMA, one of the calculated fundamental's is overestimated and the other is underestimated. In consequence, divergences are related to the sin $\times$sin gearing term rather than to the barrier. However, in DMP, the two fundamentals are slightly underestimated. The

TABLE VII. The frequencies (in cm^{-1}) for (a) dimethylamine and (b) dimethylphosphine.[a]

	$V_3'a(G_{36})$		$V_1(G_{18})$	$V_2(G_{18})$	$V_3(G_{18})$
(a)					
Mode ν_{12}					
0 0→0 1					
A_1-A_2	251.086	A_1-A_1	260.273	254.405	252.789
$G-G$	251.085	$G-G$	260.273	254.405	252.788
E_1-E_1	251.084	E_1-E_1	260.273	254.404	252.787
E_3-E_4	251.084	E_3-E_3	260.273	254.404	252.787
0 1→0 2					
A_2-A_1	247.922	A_1-A_1	254.461	250.363	248.579
$G-G$	247.932	$G-G$	254.468	250.371	248.589
E_1-E_1	247.942	E_1-E_1	254.475	250.380	248.599
E_4-E_3	247.942	E_3-E_3	254.475	250.380	248.599
0 2→0 3					
A_1-A_2	242.908	A_1-A_1	247.953	245.051	243.136
$G-G$	242.878	$G-G$	247.938	245.026	243.106
E_1-E_1	242.848	E_1-E_1	247.924	245.001	243.076
E_3-E_4	242.848	E_3-E_3	247.924	245.001	243.076
0 3→0 4					
A_2-A_1	235.977	A_1-A_1	240.327	238.099	236.021
$G-G$	235.943	$G-G$	240.293	238.078	235.985
E_1-E_1	235.910	E_1-E_1	240.259	238.058	235.951
E_4-E_3	235.906	E_3-E_3	240.257	238.054	235.946
1 0→1 1					
A_3-A_4	239.714	A_2-A_2	248.342	243.285	241.376
$G-G$	239.743	$G-G$	248.366	243.309	241.405
E_2-E_2	239.772	E_2-E_2	248.389	243.334	241.433
E_3-E_4	239.772	E_3-E_3	248.389	243.334	241.433
Mode ν_{24}					
0 0→1 0					
A_1-A_3	221.170	A_1-A_2	232.812	223.413	221.226
$G-G$	221.169	$G-G$	232.811	223.413	221.225
E_1-E_2	221.168	E_1-E_2	232.811	223.412	221.224
E_3-E_3	221.168	E_3-E_3	232.811	223.412	221.224
1 0→2 0					
A_3-A_1	216.179	A_2-A_1	225.504	218.566	216.386
$G-G$	216.198	$G-G$	225.521	218.581	216.404
E_2-E_1	216.218	E_2-E_1	225.536	218.598	216.423
E_3-E_3	216.218	E_3-E_3	225.536	218.598	216.423
2 0→3 0					
A_1-A_3	209.349	A_1-A_2	216.790	211.896	209.685
$G-G$	209.148	$G-G$	216.630	211.734	209.493
E_1-E_2	208.951	E_1-E_2	216.475	211.576	209.305
E_3-E_3	208.951	E_3-E_3	216.475	211.576	209.305
(b)					
Mode ν_{12}					
0 0→0 1					
A_1-A_2	187.696	A_1-A_1	191.298	185.617	188.098
$G-G$	187.685	$G-G$	191.289	185.604	188.087
E_1-E_1	187.673	E_1-E_1	191.990	185.591	188.075
E_3-E_4	187.673	E_3-E_3	191.990	185.591	188.075
0 1→0 2					
A_2-A_1	185.436	A_1-A_1	188.012	183.234	185.733
$G-G$	185.521	$G-G$	188.071	183.325	185.816
E_1-E_1	185.606	E_1-E_1	188.132	183.415	185.901
E_4-E_3	185.606	E_3-E_3	188.132	183.415	185.901
0 2→0 3					
A_1-A_2	181.339	A_1-A_1	182.222	178.848	181.565
$G-G$	181.073	$G-G$	182.116	178.593	181.304
E_1-E_1	180.803	E_1-E_1	182.008	178.334	181.039
E_3-E_4	180.803	E_3-E_3	182.008	178.334	181.039
0 3→0 4					
A_2-A_1	174.949	A_1-A_1	175.871	172.495	175.176
$G-G$	175.580	$G-G$	176.064	172.983	175.799
E_1-E_1	176.199	E_1-E_1	176.260	173.473	176.409
E_4-E_3	176.189	E_3-E_3	176.255	173.465	176.399
1 0→1 1					
A_3-A_4	173.930	A_2-A_2	176.052	171.348	174.226
$G-G$	174.143	$G-G$	176.261	171.589	174.437
E_2-E_2	174.352	E_2-E_2	176.462	171.822	174.642
E_3-E_4	174.352	E_3-E_3	176.462	171.822	174.642
Mode ν_{24}					
0 0→1 0					
A_1-A_3	165.508	A_1-A_2	174.953	164.848	165.929
$G-G$	165.498	$G-G$	174.944	164.837	165.918
E_1-E_2	165.487	E_1-E_2	174.934	164.825	165.909
E_3-E_3	165.487	E_3-E_3	174.934	164.825	165.902
1 0→2 0					
A_3-A_1	165.274	A_2-A_1	170.587	164.019	165.648
$G-G$	165.403	$G-G$	170.726	164.168	165.776
E_2-E_1	165.537	E_2-E_1	170.875	164.325	165.908
E_3-E_3	165.537	E_3-E_3	170.875	164.325	165.908

errors are due to the calculated barrier height which is underestimated even in the calculations with the largest basis set.

The torsional barriers of DMA and DMP were calculated to be 1201.2 and 745.0 cm^{-1} with MP2/6-31G(df,p). Recently, Durig *et al.*[1–3] and Wolrab *et al.*[9,10] have calculated the barrier heights from MW and IR data. In both molecules, the barriers fitted from IR data were found to be approximately 100 cm^{-1} lower than those obtained from MW spectroscopy.[1] In DMA,[1,9,10] this difference comes from the average of the inversion splitting performed with the MW data.[1–3,10] On the contrary, the error in DMP[2,3] derives from the geometry employed in the calculations of the kinetic energy parameters.[1,2] The improvements of the basis decrease the DMA barrier height (1201.2 cm^{-1}), whereas they introduce only barrier fluctuations around 750 cm^{-1} in DMP. Anyway, the *ab initio* DMP barrier values remain always between those obtained from MW and IR spectroscopies,[2,3] in particular, they are larger than the IR values given by Durig *et al.*[2] (700.8 and 733 cm^{-1}).

Barriers of DMA and DMP may be compared with those of dimethylether[29] (DME) and dimethyl-sulfide[30] (DMS). The barrier shape and origin of both types of molecules may be correlated. The sin×sin gearing term in DMA shows a positive sign, as in DME. This term arises from the interactions between the bending and torsion modes. It is easy to verify, during the optimization procedure, that the bending angle of both molecules does open to evade the steric effects between the methyl hydrogens. In exchange, the N–C/P–C bond-length ratio is comparable to the O–C/S–C one. The nonbonding interactions may be thus expected to be small in DMP as in DMS. Smaller steric effects give rise to lower barriers and a negative or very small sin×sin gearing term for DMP when compared with DMA.

Figure 2 show the intensities derived from c-type bands of the bc-hybrid. Selection rules in Table II relate the c-type bands with the a' mode and the a-type with the a'' mode. It can be inferred than relative intensities are well reproduced by this model. The ratio between c and a fundamental inten-

TABLE VIII. Calculated frequencies[a] and intensities[b] [MP2/6-311G(df,p)].

Assign.	Freq.	Int.	Expt.[c]	Freq.	Int.	Expt.[c]
		DMA			DMP	
Mode ν_{12}						
0 0→0 1						
A_1-A_1	252.789	3.690		188.098	0.404	
$G-G$	252.788	7.379	256.3 vs	188.087	0.807	190.4 vw
E_1-E_1	252.787	1.845		188.075	0.202	
E_3-E_3	252.787	1.845		188.075	0.202	
0 1→0 2						
A_1-A_1	248.579	2.038		185.733	0.237	
$G-G$	248.589	4.077	250.8 s	185.816	0.476	188.6 vw
E_1-E_1	248.599	1.019		185.901	0.120	
E_3-E_3	248.599	1.019		185.901	0.120	
0 2→0 3						
A_1-A_1	243.136	0.834		181.565	0.108	
$G-G$	243.106	1.657	245.3 ms	181.304	0.213	183.0 vvw
E_1-E_1	243.076	0.417		181.039	0.053	
E_3-E_3	243.076	0.417		181.039	0.053	
0 3→0 4						
A_1-A_1	236.021	0.000		175.176	0.000	
$G-G$	235.985	0.000	239.8 s	175.799	0.000	177.2 vvw
E_1-E_1	235.951	0.000		176.409	0.000	
E_3-E_3	235.946	0.000		176.399	0.000	
1 0→1 1						
A_2-A_2	241.376	0.926		174.226	0.117	
$G-G$	241.405	1.854	239.8 s	174.437	0.234	177.2 vvw
E_2-E_2	241.433	0.464		174.642	0.059	
E_3-E_3	241.433	0.464		174.642	0.059	
Mode ν_{24}						
0 0→1 0						
A_1-A_2	221.226	0.101		165.929	0.006	
$G-G$	221.225	0.203	219.4 m	165.918	0.012	169.9 vvw
E_1-E_2	221.224	0.051		165.909	0.003	
E_3-E_3	221.224	0.051		165.902	0.003	
1 0→2 0						
A_2-A_1	216.386	0.023		165.929	0.003	
$G-G$	216.404	0.046	213.0 w	165.776	0.005	166.1 vvw
E_2-E_1	216.423	0.012		165.908	0.002	
E_3-E_3	216.423	0.012		165.908	0.002	

[a]In cm^{-1}.
[b]$\times 10^{-4}$.
[c]vs=very strong; s=strong; ms=medium strong; w=weak; vw=very weak; vvw=very very weak.

sities was found 36.44 for DMA and 34.94 for DMP. Intensities are stronger in DMA than in DMP.

The first and second sequences of the a' mode in DMA were calculated to be 248.589 and 243.106 cm^{-1} with the largest basis set. The differences between calculated and experimental bands[1] are -2.2 cm^{-1}. Corresponding values for the a' mode were determined to be 216.404 and 209.493 cm^{-1}. Divergences are equal to $+3.4$ and $+6.8$ cm^{-1}. In DMP, the calculated values were 185.816 and 181.304 cm^{-1} for the a' mode and 165.918 and 165.776 cm^{-1} for a''. It can be deduced that the main diagonal of the potential surface (where $\theta_1=\theta_2$) related to the a'' mode is well described in the calculations, whereas the secondary diagonal is not so well reproduced.

Durig *et al.*[1] have assigned the IR band of DMA at 239.8 cm^{-1} to the third sequence of the a' mode. This assignment have to be supported by the intensities. The observed intensity of this band, however, is unusually stronger than the second sequence one, whereas the calculated intensity is relatively weak. If one remarks that the calculated a' third sequence and the 10→11 (a'' torsionally excited a' funda-

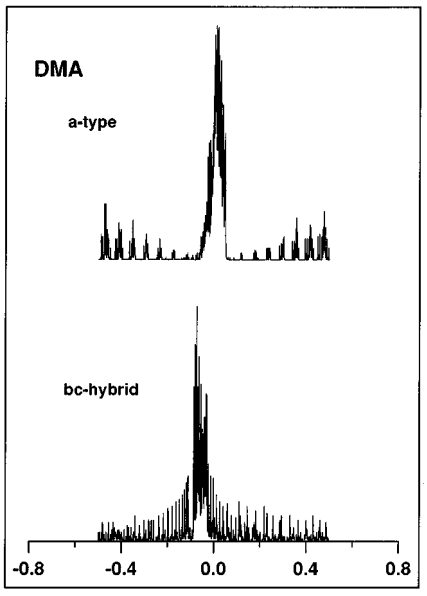

FIG. 2. The rotational contours for the single degenerate A component simulated for a-type $A_1(00)\rightarrow A_2(10)$ and bc-hybrid $A_1(00)\rightarrow A_1(01)$ bands of dimethylamine.

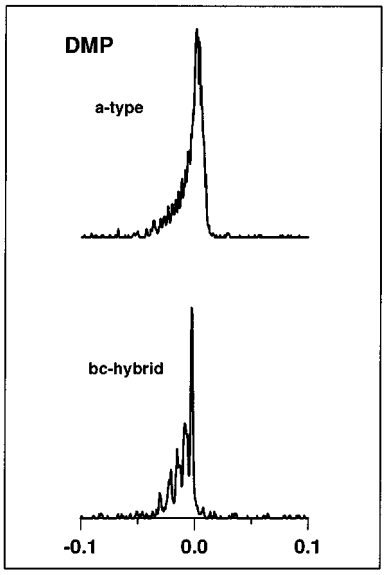

FIG. 3. The rotational contours for the single degenerate A component simulated for a-type $A_1(00)\rightarrow A_2(10)$ and bc-hybrid $A_1(00)\rightarrow A_1(01)$ bands of dimethylphosphine.

mental) transitions are found approximately at the same frequency (taking into account that the theoretical values for the a'' levels are found 2 cm^{-1} too high), the 239.8 cm^{-1} band could be due thus the superimposition of both transitions. The observed band at 235.0 cm^{-1}, assigned to the $10\rightarrow 11$ transition by Durig *et al.* could be reassigned to the $21\rightarrow 11$ overtone. The Raman band observed at 476 cm^{-1} attached with the $01\rightarrow 12$ overtone (approx $239.8+235.0$) does agree with this reassignment.

In DMP[2], the band observed at 177.2 cm^{-1} contains in the same way the a' third sequence and the $10\rightarrow 11$ transitions. The experimental relative intensities support also this assignment.

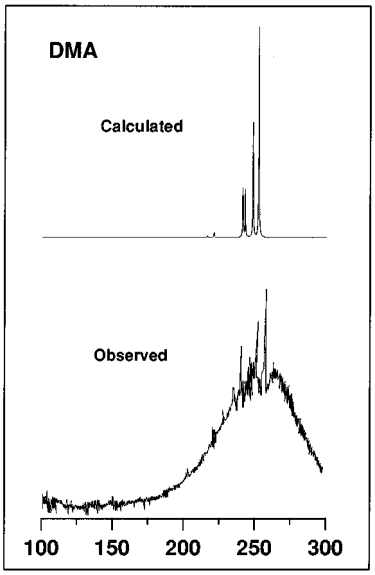

FIG. 4. Observed and calculated far infrared spectra of dimethylamine. Observed spectrum is from Ref. 1.

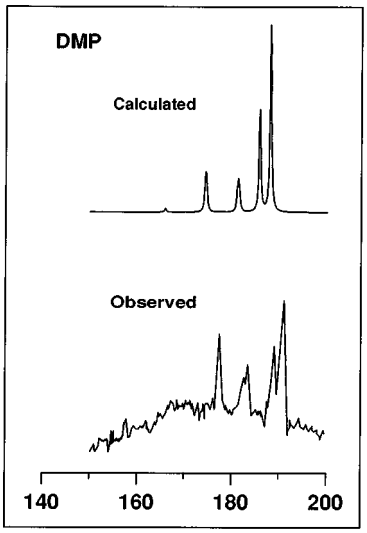

FIG. 5. Observed and calculated far infrared spectra of dimethylphosphine. Observed spectrum is from Ref. 2.

In the present paper, the *ab initio* calculations appear to be an useful tool to evaluate the effects of the extra potential energy (and kinetic) terms on the band locations. These terms change drastically the symmetry properties of the Hamiltonian operator. The energy levels of Tables IV and V are calculated from one G_{36} and three G_{18} different potential energy functions. It is shown that the effects on the energy levels are relatively small. Calculations confirm generally the assignments performed with the experimental potentials fitted with only five terms. The calculations, however, allow to reassign the observed band at 239.8 cm^{-1} in DMA and 177.2 cm^{-1} in DMP to the superimposition of two different transitions: the third sequence and a vibrationally excited fundamental.

ACKNOWLEDGMENTS

This work has been supported by the European Union under the Human Capital and Mobility Scheme (contract CHRZ CT 93-0157). The authors also acknowledge the financial assistance from the ''Comision Interministerial de Ciencias y Technologia'' of Spain through grant no. PB 93-0185.

[1] J. R. Durig, M. G. Griffin, and P. Groner, J. Phys. Chem. **81**, 554 (1977).
[2] J. R. Durig, M. G. Griffin, and W. J. Natter, J. Phys. Chem. **81**, 1588 (1977).
[3] J. R. Durig, P. Groner, and Y. S. Li, J. Chem. Phys. **67**, 2216 (1977).
[4] J. G. Aston, M. L. Edinoff, and W. S. Forster, J. Am. Chem. Soc. **61**, 1539 (1939).
[5] J. R. Barcelo and J. Bellanato, Spectrochim. Acta **8**, 27 (1956).
[6] W. G. Fateley and F. A. Miller, Spectrochim. Acta **18**, 977 (1962).
[7] K. D. Möller, A. R. De Meo, D. R. Smith, and L. H. London, J. Chem. Phys. **47**, 2609 (1967).
[8] G. Dellepiane and G. Zerbi, J. Chem. Phys. **48**, 3573 (1968).
[9] J. E. Wollrab and V. W. Laurie, J. Chem. Phys. **48**, 5058 (1968).
[10] J. E. Wollrab and V. W. Laurie, J. Chem. Phys. **54**, 532 (1971).

[11] G. Gamer and H. Wolff, Spectrochim. Acta Part A **29**, 129 (1973).
[12] Y. G. Smeyers, A. Huertas-Cabrera, Theor. Chim. Acta **64**, 97 (1983).
[13] Y. G. Smeyers, M. Fernandez, and V. Botella, J. Mol. Struct. (Teochem) **210**, 273 (1990).
[14] K. Siam, C. Van Alsenoy, and L. Schåfer, J. Mol. Struct. (Teochem) **209**, 387 (1990).
[15] D. Consalvo, J. W. I. van Bladel, R. Engeln, and J. Reuss, Chem. Phys. **171**, 221 (1993).
[16] H. C. Beachell and B. Katlafsky, J. Chem. Phys. **27**, 182 (1957).
[17] L. S. Bartell, J. Chem. Phys. **32**, 832 (1960).
[18] T. Kojima, E. L. Breig, and C. C. Lin, J. Chem. Phys. **6**, 2139 (1961).
[19] R. Nelson, J. Chem. Phys. **39**, 2382 (1963).
[20] J. R. Durig and J. E. Saunders, J. Raman. Spectrosc. **4**, 121 (1975).
[21] P. C. Fox, J. P. Bowen, and N. L. Allinger, J. Am. Chem. Soc. **114**, 8536 (1992).
[22] M. Kreglewski, in *Structure and Conformations of Non-Rigid Molecules*, NATO ASI Series C, edited by J. Laane (Kluwer Academic, The Netherlands, 19XX), Vol. 410, p. 29.
[23] D. R. Lide, Jr. and D. E. Mann, J. Chem. Phys. **28**, 572 (1958).
[24] T. Kojima, E. L. Breig, and C. C. Lin, J. Chem. Phys. **35**, 2139 (1961).
[25] D. C. Moule, Y. G. Smeyers, M. L. Senent, D. J. Clouthier, J. Karolczak, and R. Judge, J. Chem. Phys. **95**, 3137 (1991).
[26] Y. G. Smeyers, M. L. Senent, V. Botella, and D. C. Moule, J. Chem. Phys. **98**, 2754 (1993).
[27] M. L. Senent, D. C. Moule, Y. G. Smeyers, A. Toro-Labbé, and F. J. Peñalver, J. Mol. Spectrosc. **164**, 66 (1994).
[28] M. L. Senent, D. C. Moule, and Y. G. Smeyers, Can. J. Phys. **73**, 425 (1995).
[29] M. L. Senent, D. C. Moule, and Y. G. Smeyers, J. Chem. Phys. **102**, 5952 (1995).
[30] M. L. Senent, D. C. Moule, and Y. G. Smeyers, J. Phys. Chem. **99**, 7970 (1995).
[31] M. L. Senent, D. C. Moule, and Y. G. Smeyers, J. Mol. Struct. **372**, 257 (1996).
[32] Y. G. Smeyers, J. Mol. Struct. **107**, 3 (1984).
[33] Y. G. Smeyers and A. Niño, J. Comput. Chem. **8**, 380 (1987).
[34] Y. G. Smeyers, in *Advances in Quantum Chemistry*, edited by P. O. Lowden (Academic, New York, 1992), Vol. 24, pp 1–77.
[35] Y. G. Smeyers and M. N. Bellido, Int. J. Quantum Chem **19**, 553 (1981).
[36] Y. G. Smeyers and A. Hernández-Laguna, Int. J. Quantum Chem. **22**, 681 (1982).
[37] GAUSSIAN 92, M. J. Frisch, G. W. Trucks, M. Head-Gordon, P. M. W. Gill, M. W. Wong, J. B. Foresman, B. G. Johnson, H. B. Schlegel, M. A. Robb, E. S. Repongle, R. Gomperts, J. L. Andres, K. Raghavachari, J. S. Binkley, C. Gonzalez, R. L. Martin, D. J. Fox, D. J. Defrees, J. Baker, J. J. P. Steward and J. A. Pople (Gaussian, Inc., Pittsburg PA, 1992).
[38] R. H. Judge, Comput. Phys. Commun. **47**, 361 (1987).